FoxO6 Integrates Insulin Signaling With Gluconeogenesis in the Liver

Dae Hyun Kim,[1] German Perdomo,[1] Ting Zhang,[1] Sandra Slusher,[1] Sojin Lee,[1] Brett E. Phillips,[1] Yong Fan,[1] Nick Giannoukakis,[1] Roberto Gramignoli,[2] Stephen Strom,[2] Steven Ringquist,[1] and H. Henry Dong[1]

OBJECTIVE—Excessive endogenous glucose production contributes to fasting hyperglycemia in diabetes. This effect stems from inept insulin suppression of hepatic gluconeogenesis. To understand the underlying mechanisms, we studied the ability of forkhead box O6 (FoxO6) to mediate insulin action on hepatic gluconeogenesis and its contribution to glucose metabolism.

RESEARCH DESIGN AND METHODS—We characterized FoxO6 in glucose metabolism in cultured hepatocytes and in rodent models of dietary obesity, insulin resistance, or insulin-deficient diabetes. We determined the effect of FoxO6 on hepatic gluconeogenesis in genetically modified mice with FoxO6 gain-versus loss-of-function and in diabetic *db/db* mice with selective FoxO6 ablation in the liver.

RESULTS—FoxO6 integrates insulin signaling to hepatic gluconeogenesis. In mice, elevated FoxO6 activity in the liver augments gluconeogenesis, raising fasting blood glucose levels, and hepatic FoxO6 depletion suppresses gluconeogenesis, resulting in fasting hypoglycemia. FoxO6 stimulates gluconeogenesis, which is counteracted by insulin. Insulin inhibits FoxO6 activity via a distinct mechanism by inducing its phosphorylation and disabling its transcriptional activity, without altering its subcellular distribution in hepatocytes. FoxO6 becomes deregulated in the insulin-resistant liver, accounting for its unbridled activity in promoting gluconeogenesis and correlating with the pathogenesis of fasting hyperglycemia in diabetes. These metabolic abnormalities, along with fasting hyperglycemia, are reversible by selective inhibition of hepatic FoxO6 activity in diabetic mice.

CONCLUSIONS—Our data uncover a FoxO6-dependent pathway by which the liver orchestrates insulin regulation of gluconeogenesis, providing the proof-of-concept that selective FoxO6 inhibition is beneficial for curbing excessive hepatic glucose production and improving glycemic control in diabetes. *Diabetes* **60:2763–2774, 2011**

G luconeogenesis is a life-sustaining process for maintaining blood glucose levels within the physiologic range and providing the sole fuel source for the brain, testes, and erythrocytes during starvation. Gluconeogenesis takes place mainly in the liver in a metabolic pathway that is tightly regulated by insulin. When hepatic insulin signaling goes awry, gluconeogenesis becomes unabated, resulting in excessive glucose production and contributing to fasting hyperglycemia in diabetes.

The molecular basis that couples impaired insulin action to unrestrained gluconeogenesis remains incompletely defined. Previous studies characterize forkhead box O1 (FoxO1) as a key transcription factor for mediating insulin action on gluconeogenesis (1–3). FoxO1 binds as a *trans*-activator to the promoters of PEPCK and glucose-6-phosphatase (G6Pase) for stimulating gluconeogenic gene expression. This effect is amplified by proliferator-activated receptor-γ coactivator-1α, which acts as a coactivator for augmenting FoxO1 activity in promoting gluconeogenesis during fasting (4).In response to postprandial insulin release, FoxO1 is phosphorylated by Akt/protein kinase B (PKB), resulting in its nuclear exclusion and in inhibition of gluconeogenesis (1,2,5). These data underscore the importance of FoxO1 in integrating hepatic insulin signaling with gluconeogenesis.

However, FoxO1 depletion in the liver does not abolish insulin regulation of gluconeogenesis (6). In keeping with this observation, we show that FoxO1-deficient mice are associated with diminished gluconeogenesis and an impaired ability to maintain fasting euglycemia (7). Loss of FoxO1 function attenuates, but does not abrogate, the responsiveness of the liver to insulin (6–9), spurring the hypothesis that additional factors integrate insulin signaling to gluconeogenesis in the liver.

To deepen our understanding of the mechanism underlying insulin-dependent regulation of gluconeogenesis, we studied the ability of FoxO6 to mediate the inhibitory effect of insulin on gluconeogenesis in the liver. FoxO6 is a nuclear transcription factor that is classified to the Fox O family. Because of scant data on FoxO6 in the literature, little is known about its role in metabolism and its impact on diabetes. We showed that FoxO6 was expressed in human and rodent livers. Hepatic FoxO6 expression was maintained at low basal levels in fed states and was significantly induced at mRNA and protein levels in mice after an overnight fast. FoxO6 targeted the G6Pase gene for *trans*-activation, contributing to augmented gluconeogenesis in the liver. This effect was enhanced by glucagon (via cAMP) and inhibited by insulin. Insulin stimulated FoxO6 phosphorylation and disabled its DNA-binding activity without altering its subcellular distribution in hepatocytes.

Transgenic mice expressing a constitutively active FoxO6 allele in the liver were associated with premature onset of metabolic syndrome, culminating in the development of fasting hyperglycemia, fasting hyperinsulinemia, and glucose intolerance. In contrast, hepatic FoxO6 depletion diminished the ability of the liver to manufacture glucose, resulting in fasting hypoglycemia in mice. Furthermore, FoxO6 became deregulated, accounting for its
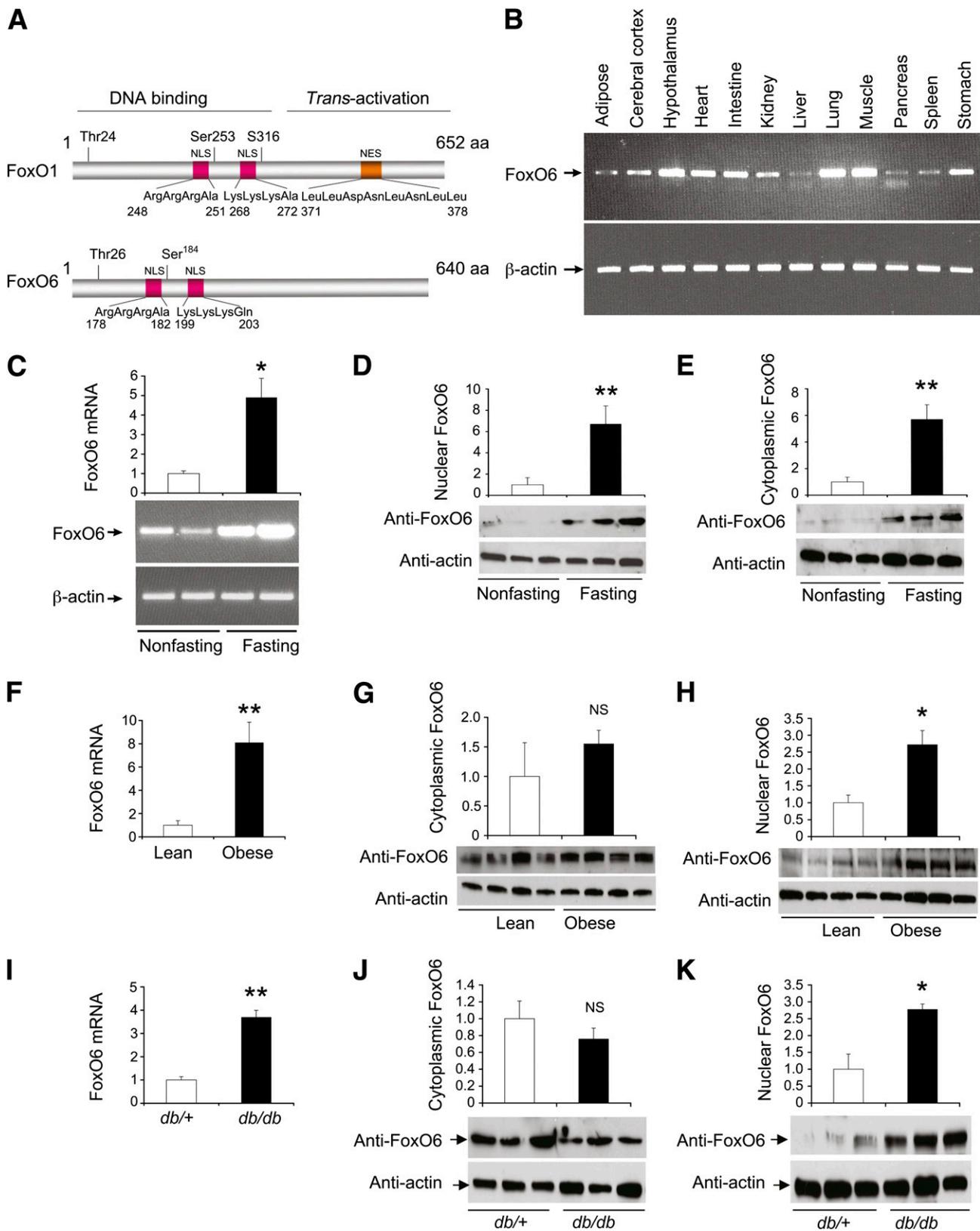
FIG. 1. Characterization of FoxO6 and its hepatic expression under physiologic and pathologic conditions. *A*: FoxO6 is divergent from FoxO1. FoxO6 contains 640 amino acid (aa) residues and two Akt/PKB phosphorylation sites, lacking NES. NLS, nuclear localization signal. *B*: FoxO6 is ubiquitously expressed. C57BL/6J male mice (aged 10 weeks) were killed under fed conditions for collecting tissues (20 mg), which were subjected to RT-PCR analysis using FoxO6 and β-actin primers. Data were representative of three independent assays from three mice. C57BL/6J male mice (aged 10 weeks, $n = 3$) were killed under fed conditions or after a 16-h fast. *C*: Total liver RNA was subjected to real-time quantitative (q) RT-PCR assay using FoxO6 and β-actin primers. Total liver proteins were separated into nuclear (*D*) and cytoplasmic (*E*) fractions, which were analyzed by immunoblot assay using anti-FoxO6 antibody. Furthermore, C57BL/6J male mice (aged 6 weeks) were rendered obese after 8 weeks of high-fat feeding. Mice in groups fed regular chow ($n = 6$, body wt 26.5 ± 2.1 g) and a high-fat diet ($n = 6$, 51.4 ± 4.9 g) were killed after a 16-h fast. *F*: Total liver RNA was subjected to real-time qRT-PCR assay for determining hepatic FoxO6 mRNA levels. Total liver proteins were separated into

unchecked activity in promoting gluconeogenesis in the insulin-resistant liver, consistent with the development of fasting hyperglycemia in diabetic *db/db* mice.

These abnormalities in gluconeogenesis, along with fasting hyperglycemia, were reversible in response to small interfering RNA (siRNA)-mediated hepatic FoxO6 knockdown in diabetic *db/db* mice. Our data characterize FoxO6 as an important transcription factor that independently integrates insulin signaling to hepatic gluconeogenesis. The gluconeogenic pathway has been a major target for antihyperglycemia therapies in diabetes. Our findings provide the proof-of-concept that selective FoxO6 inhibition is beneficial for curbing excessive hepatic glucose production and improving glycemic control in diabetes.

RESEARCH DESIGN AND METHODS

Animal studies. CD1 mice (aged 6 weeks) were obtained from Charles River Laboratory (Wilmington, MA). C57BL/6J, *db/db*, and heterozygous *db/+* mice (aged 8 weeks) were purchased from The Jackson Laboratory (Bar Harbor, ME). Mice were fed standard rodent chow and water ad libitum and kept in sterile cages with a 12-h light/dark cycle. To induce obesity, mice were fed a high-fat diet (fat content >60 kcal%; Research Diets, Inc., New Brunswick, NJ) for 8 weeks, as described previously (10). For blood chemistry, mice were fasted for 16 h, and tail vein blood samples were collected into capillary tubes precoated with potassium-EDTA (Sarstedt, Nümbrecht, Germany) for the determination of blood glucose levels using Glucometer Elite (Bayer Healthcare LLC, Mishawaka, IN) or plasma insulin levels using the ultrasensitive mouse insulin enzyme-linked immunosorbent assay (ALPCO, Windham, NH), as described previously (7,11). All procedures were approved by the University of Pittsburgh Institutional Animal Care and Use Committee.
Glucose tolerance test. Mice were fasted for 16 h, followed by an intraperitoneal injection of glucose at the dose of 2 g/kg body wt, as described previously (10).
Pyruvate tolerance test. Mice were fasted for 16 h, followed by intraperitoneal injection of pyruvate at the dose of 2 g/kg body wt, as described previously (12).
Insulin tolerance test. Mice were injected intraperitoneally with regular human insulin (Eli Lilly, Indianapolis, IN) at the dose of 0.75 IU/kg body wt, as described previously (10).
Microsome preparation. Liver tissue (40 mg) was homogenized in 400 μL microsome buffer (20 mmol/L Tris-Cl, pH 7.0, 1 mmol/L EDTA, 0.25 mol/L sucrose). After centrifugation at 4,000g for 10 min, the supernatant was transferred into an ultracentrifuge tube (Part No. S300535A; Hitachi Koki Co., Hitachi, Japan) and was centrifuged at 100,000 rpm for 30 min in the Sorvall Discovery M150SE ultracentrifuge (Hitachi Koki Co.). The pellets were resuspended in microsome buffer (500 μL). To prepare microsomes from cultured hepatocytes, 1×10^6 cells were suspended in mammalian protein extraction reagent (100 μL; Pierce, Rockford, IL) containing Halt protease inhibitor cocktail (1 μL; Pierce). Microsome buffer (200 μL) was added, and cells were lysed by vigorous vortexing, followed by centrifugation at 4,000g for 10 min. The supernatant was used for the preparation of microsomes by ultracentrifugation.
G6Pase activity assay. G6Pase catalyzes the conversion of glucose-6-phosphate to glucose and phosphorus (Pi), the final step of gluconeogenesis. To determine G6Pase activity, 50 μL microsomes (protein concentration, 500 μg/mL) were mixed with 100 μL G6Pase assay buffer (1% ammonium molybdate solution made in 5 mol/L H_2SO_4, 5% ferrous sulfate heptahydrate made in phosphate-buffered saline) and 50 μL glucose-6-phosphate (200 mmol/L) in a total volume of 200 μL in a 96-well microplate. In the same microplate, aliquots of Pi solution (650 mmol/L KH_2PO_4) were mixed with 100 μL G6Pase assay buffer in a fixed volume of 200 μL/well to yield a series of Pi concentrations (30–150 μmol/L) for determining a standard curve, defined as the amount of Pi as a function of optical density at 660 nm. As negative control, three wells without microsomes were included in the same microplate. After incubation at 37°C for 15 min, the optical density of individual wells was determined at 660 nm.

G6Pase activity is defined as the production of Pi (in micromoles) per unit time (in minutes) per microgram of cellular microsomes.
Statistics. Statistical analyses of data were performed by ANOVA using StatView software (Abacus Concepts, Berkeley, CA). ANOVA post hoc tests were used to perform pairwise comparisons to study the significance among different conditions. Data are expressed as the mean ± SEM. Values of $P < 0.05$ were considered statistically significant. Other methods are described in the Supplementary Data.

RESULTS

Hepatic FoxO6 expression under physiologic and pathologic conditions. FoxO6 consists of an amino DNA-binding domain and a carboxyl *trans*-activation domain, a structural feature that is characteristic of the FoxO family. However, FoxO6 differs from other members of FoxO family in fundamental ways (Fig. 1*A*): *1*) FoxO6 has the lowest degree of homology (<30%) in amino acid sequence with other members of the FoxO family. *2*) FoxO6 contains only two consensus Akt/PKB phosphorylation sites (Thr[26] and Ser[184]) within its amino DNA-binding domain. In contrast, other members of FoxO family contain three highly conserved phosphorylation sites (Thr[24], Ser[256], and Ser[319] in FoxO1). *3*) FoxO6 lacks the nuclear export signal (NES), a motif that is conserved in other members of the FoxO family. We determined FoxO6 tissue distribution, demonstrating that FoxO6 was ubiquitously expressed in mice (Fig. 1*B*). Such a broad tissue distribution of FoxO6 presages a wide spectrum of FoxO6 function in different organs. However, because of scant data on FoxO6 in the literature, little is known about its role in metabolism in response to nutritional cues.

Here we focused on the characterization of FoxO6 in glucose metabolism, with a central hypothesis that FoxO6 integrates insulin signaling with gluconeogenesis in the liver. To associate FoxO6 function with hepatic metabolism, we determined FoxO6 expression in the liver under physiologic and pathologic conditions. Hepatic FoxO6 expression was maintained at low basal levels in fed states and was markedly induced in mice after an overnight fast (Fig. 1*C–E*). Likewise, hepatic FoxO6 mRNA and its nuclear protein levels were significantly upregulated, correlating with the pathogenesis of fasting hyperglycemia in dietary obese mice (Fig. 1*F–H*) and diabetic *db/db* mice (Fig. 1*I–K*). Significantly higher FoxO6 mRNA and its nuclear protein levels were also detected in the insulin-deficient liver, coinciding with the episode of fasting hyperglycemia in streptozotocin-induced diabetic mice (Supplementary Fig. 1). Thus, insulin resistance and insulin deficiency were invariably associated with FoxO6 overproduction, raising the postulation that FoxO6 activity is inhibited by insulin and that loss of insulin inhibition is attributable to FoxO6 deregulation in diabetes.
Insulin regulation of hepatic FoxO6 activity. To address the above hypothesis, we studied hepatic regulation of FoxO6 expression by insulin in cultured human primary hepatocytes. Hepatic FoxO6 expression was upregulated by cAMP/dexamethasone (Fig. 2*A*), correlating with the induction of G6Pase (Fig. 2*B*) and PEPCK (Fig. 2*C*), two key enzymes in gluconeogenesis. This effect was reversed

---

cytoplasmic (*G*) and nuclear (*H*) fractions, which were analyzed by anti-FoxO6 immunoblot assay. Likewise, male diabetic *db/db* (*n* = 8, aged 6 months; blood glucose levels, 62.8 ± 3.9 mg/dL) vs. male age-matched control *db/+* mice (*n* = 8, 310 ± 28 mg/dL) were killed after a 16-h fast, and liver tissue was processed for the preparation of cytoplasmic and nuclear fractions. *I*: Total liver RNA was subjected to real-time qRT-PCR assay for determining hepatic FoxO6 mRNA levels. Aliquots of cytoplasmic (*J*) and nuclear (*K*) proteins (20 μg) were subjected to semiquantitative immunoblot analysis for FoxO6. *P < 0.05 and **P < 0.005 vs. control by ANOVA; NS, not significant. (A high-quality color representation of this figure is available in the online issue.)
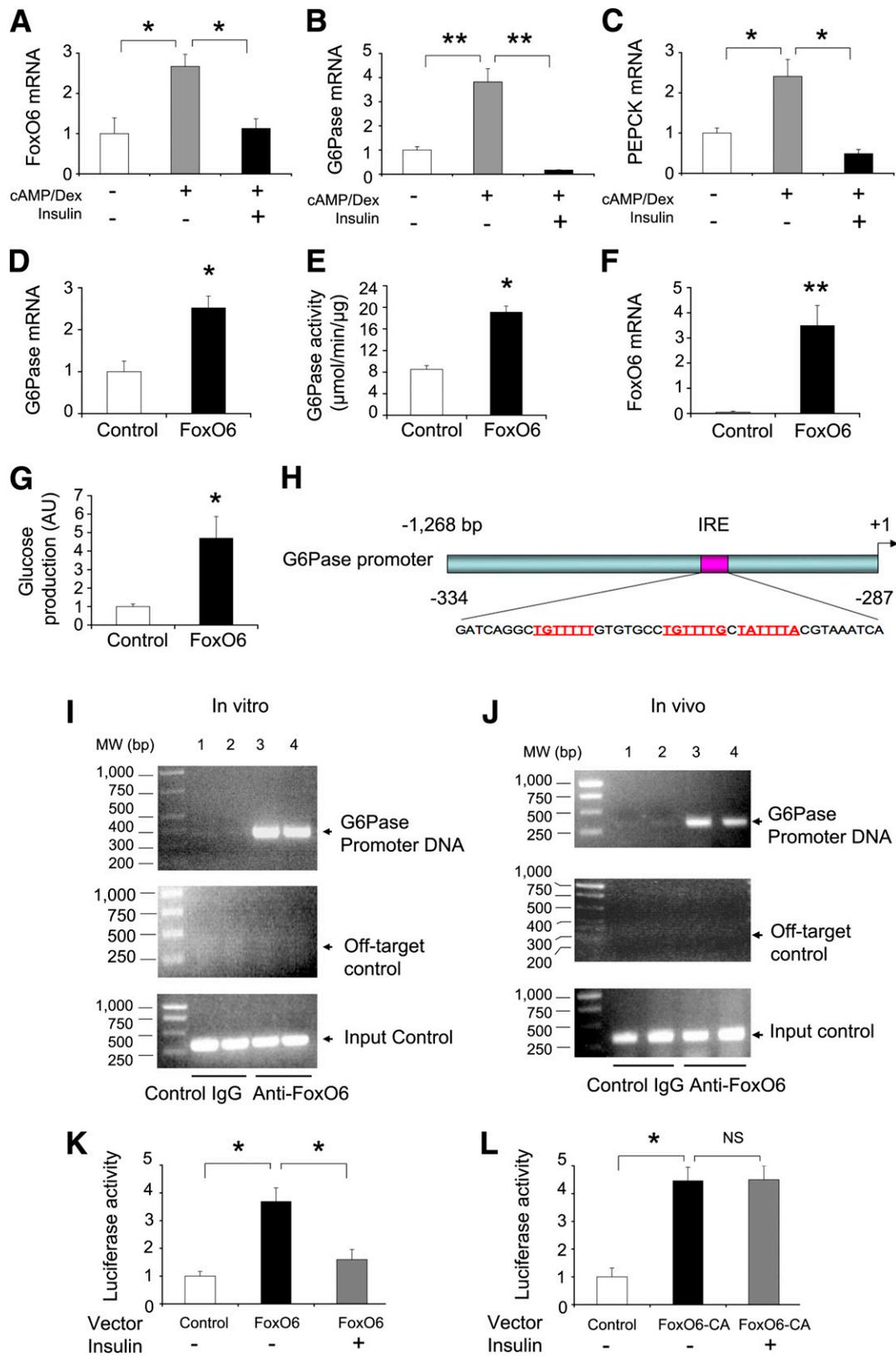
FIG. 2. Insulin regulation of FoxO6 transcriptional activity. Human primary hepatocytes were cultured in the absence or presence of 8-cpt-cAMP (cAMP analog, 500 μmol/L) and dexamethasone (Dex, 100 μmol/L), with and without the inclusion of insulin (100 nmol/L). After 24-h incubation, cells were subjected to real-time quantitative (q) RT-PCR assay for determination of FoxO6 mRNA levels (*A*), G6Pase mRNA levels (*B*), and PEPCK mRNA levels (*C*). In addition, HepG2 cells were transduced with control and FoxO6 vectors at a fixed dose (100 plaque-forming units [pfu]/cell). After 24-h incubation, cells were replenished with glucose-free glutamine-containing Dulbecco's modified Eagle's medium that was supplemented with 1 mmol/L pyruvate. After 6-h incubation, conditioned medium was used for determination of glucose. Cells were subjected to real-time qRT-PCR analysis and anti-FoxO6 immunoblot assay using anti-actin antibody as control. *D*: G6Pase mRNA levels. *E*: Hepatic G6Pase activity. *F*: FoxO6 mRNA levels. *G*: Glucose levels in the medium. AU, arbitrary unit. *H*: The mouse G6Pase promoter contains three tandem copies of the insulin-responsive element (IRE). This 1.2-kb G6Pase promoter was cloned in the luciferase reporter expression vector pG6P-Luc. *I*: FoxO6 binds

by insulin, suggesting that hepatic FoxO6 activity is induced by glucagon (via cAMP) and inhibited by insulin.

FoxO6 targets G6Pase gene for *trans*-activation. To address the hypothesis that FoxO6 targets the G6Pase gene for *trans*-activation, we determined the ability of FoxO6 to stimulate G6Pase expression in HepG2 cells. Hepatic FoxO6 production significantly raised G6Pase mRNA expression (Fig. 2D) and G6Pase activity (Fig. 2E), correlating with a threefold elevation of FoxO6 mRNA levels in FoxO6 vector-transduced HepG2 cells (Fig. 2F). This effect translated into a marked induction of glucose production, as proven by a fivefold elevation in glucose concentrations in conditioned medium of HepG2 cells expressing FoxO6 (Fig. 2G). Similar results were reproduced in cultured mouse primary hepatocytes (Supplementary Fig. 2). Moreover, FoxO6 was shown to bind to the conserved insulin-responsive element ($-334/-287$ base pairs) in the G6Pase promoter (Fig. 2H), as detected by chromatin immunoprecipitation assay. This finding was reproduced in HepG2 cells (Fig. 2I) and in the livers of fasted mice (Fig. 2J).

FoxO6 activity is subject to insulin inhibition. To address the hypothesis that hepatic FoxO6 activity is subject to insulin inhibition, we transferred the G6Pase promoter-directed luciferase reporter system into HepG2 cells in the presence or absence of FoxO6 production, demonstrating that FoxO6 stimulated G6Pase promoter activity and that this effect was counteracted by insulin (Fig. 2K). As a control, we generated an adenoviral vector expressing a constitutively active allele of FoxO6 (FoxO6-CA) by converting the conserved Akt/PKB phosphorylation site at Ser[184] to Ala[184] (Supplementary Fig. 3). FoxO6-CA stimulated G6Pase promoter activity, but its stimulatory effect on G6Pase promoter activity was refractory to insulin inhibition (Fig. 2L). This action correlated with the inability of insulin to phosphorylate and inhibit FoxO6-CA mutant activity (Supplementary Fig. 4). In contrast, wild-type FoxO6 underwent insulin-stimulated phosphorylation in cultured HepG2 cells and in the livers of mice (Supplementary Fig. 4).

As additional control, we determined the specificity of our anti–phospho-FoxO6 antibody. This polyclonal antibody was derived against a peptide of 14 amino acid residues (corresponding to amino acid 182–195 of the mouse FoxO6 protein) with Ser[184] phosphorylated. Our anti–phospho-FoxO6 antibody reacted selectively with phosphorylated FoxO6 protein in the livers of mice that were pretreated with insulin (Supplementary Fig. 4C). In the same assay, our anti–phospho-FoxO6 antibody was negative in cross-reactivity with other members in the FoxO family (Supplementary Fig. 5).

Effect of FoxO6 on hepatic gluconeogenesis. To provide in vivo evidence that FoxO6 targets the G6Pase promoter for *trans*-activation, we transferred adenoviral vectors

encoding the G6Pase promoter-directed luciferase reporter system along with the Adv-FoxO6-CA or Adv-null vector into CD1 mice ($n = 10$ per group), followed by whole-body imaging (Fig. 3A). This assay detected a significant induction of hepatic luciferase activity, defined by the luminescent radiance in the liver with FoxO6-CA production (Fig. 3B). This result was confirmed by determination of luciferase activity in the liver protein extracts of FoxO6-CA vector-treated mice (Fig. 3C). Consistent with its role in gluconeogenesis, FoxO6-CA augmented hepatic PEPCK mRNA (Fig. 3D) and PEPCK protein (Fig. 3E), as well as G6Pase mRNA expression (Fig. 3F), correlating with increased FoxO6 production in the liver (Fig. 3G). This effect contributed to augmented gluconeogenesis, as proven by significantly higher blood glucose levels in FoxO6-CA vector-treated mice after an intraperitoneal dose of pyruvate solution (Fig. 3H). Mice with hepatic FoxO6-CA production were associated with elevated fasting blood glucose (Fig. 3I) and plasma insulin levels (Fig. 3J), accompanied by impaired glucose tolerance (Fig. 3K). No differences were seen in body weight between FoxO6-CA and control groups (Fig. 3L). These data support the idea that FoxO6 targets the G6Pase gene for *trans*-activation, contributing to the induction of hepatic gluconeogenesis. As a control, we determined the potential effect of FoxO6 on hepatic expression of other members in the FoxO family. No significant differences in hepatic FoxO1, FoxO3, and FoxO4 mRNA levels were detected in control versus FoxO6-CA groups (Supplementary Fig. 6), precluding the possibility that the observed induction of hepatic gluconeogenesis was secondary to altered production of other FoxO proteins in FoxO6-CA mice.

Mechanism of insulin inhibition of FoxO6 activity. FoxO6, although phosphorylated in response to insulin, did not undergo insulin-dependent nuclear exclusion in HepG2 cells, as determined by immunohistochemistry (Fig. 4A). In contrast, FoxO1 was translocated from the nucleus to the cytoplasm in the presence of insulin. To consolidate these findings, we determined FoxO6 subcellular distribution in the absence or presence of constitutively active Akt (Akt-CA), which has been shown to phosphorylate its targets independently of insulin (13). FoxO6 remained predominantly in the nucleus regardless of Akt-CA in HepG2 cells (Fig. 4B). Using the same assay, we previously showed that Akt-CA stimulates FoxO1 phosphorylation and promotes its trafficking from the nucleus to cytoplasm (7). It follows that insulin inhibits FoxO6 activity by a distinct mechanism that is different from other members of the FoxO family.

To probe the underlying mechanism, we performed chromatin immunoprecipitation assay to probe the molecular interaction between FoxO6 and the G6Pase promoter DNA. FoxO6 associated with the G6Pase promoter DNA in fasted livers (Fig. 4C), correlating with the stimulatory effect

to the G6Pase promoter in HepG2 cells. HepG2 cells were transfected with pG6P-Luc in the presence of FoxO6 vector at 50 pfu/cell in duplicate. After 24-h incubation, cells were subjected to chromatin immunoprecipitation (ChIP) assay using rabbit preimmune IgG (*lanes 1* and *2*) or anti-FoxO6 antibody (*lanes 3* and *4*). Immunoprecipitates were subjected to PCR analysis using a pair of primers flanking the IRE sequence ($-471/-122$ nucleotide [nt]) in the G6Pase promoter. As a negative control, the immunoprecipitates were analyzed using a pair of off-target primers flanking the G6Pase coding region (684–1,074 nt). As a positive control, aliquots of input DNA samples (3 μL) were used in PCR analysis. *J*: FoxO6 binds to the G6Pase promoter in the liver. CD-1 mice ($n = 4$) were killed after a 16-h fast. Liver tissues were subjected to ChIP assay using rabbit preimmune IgG (*lanes 1* and *2*) or anti-FoxO6 antibody (*lanes 3* and *4*). Furthermore, HepG2 cells were transfected with 1 μg of the plasmid encoding the G6Pase promoter-directed luciferase reporter system in the presence of FoxO6 (*K*) or its constitutively active allele FoxO6-CA (*L*) production. Adv-FoxO6, Adv-FoxO6-CA, and control Adv-null vectors were used at a fixed dose (50 pfu/cell). Cells were incubated for 24 h in the presence or absence of insulin (100 nmol/L), followed by luciferase assay. To normalize the transfection efficiency, 1 μg of pCA35-LacZ encoding β-galactosidase was included in each transfection. The promoter activity, defined as the ratio between luciferase and β-galactosidase activities, was determined. Data were from 4 to 6 independent experiments. *$P < 0.05$ and **$P < 0.001$ vs. control by ANOVA; NS, not significant. bp, base pairs; MW, molecular weight. (A high-quality color representation of this figure is available in the online issue.)
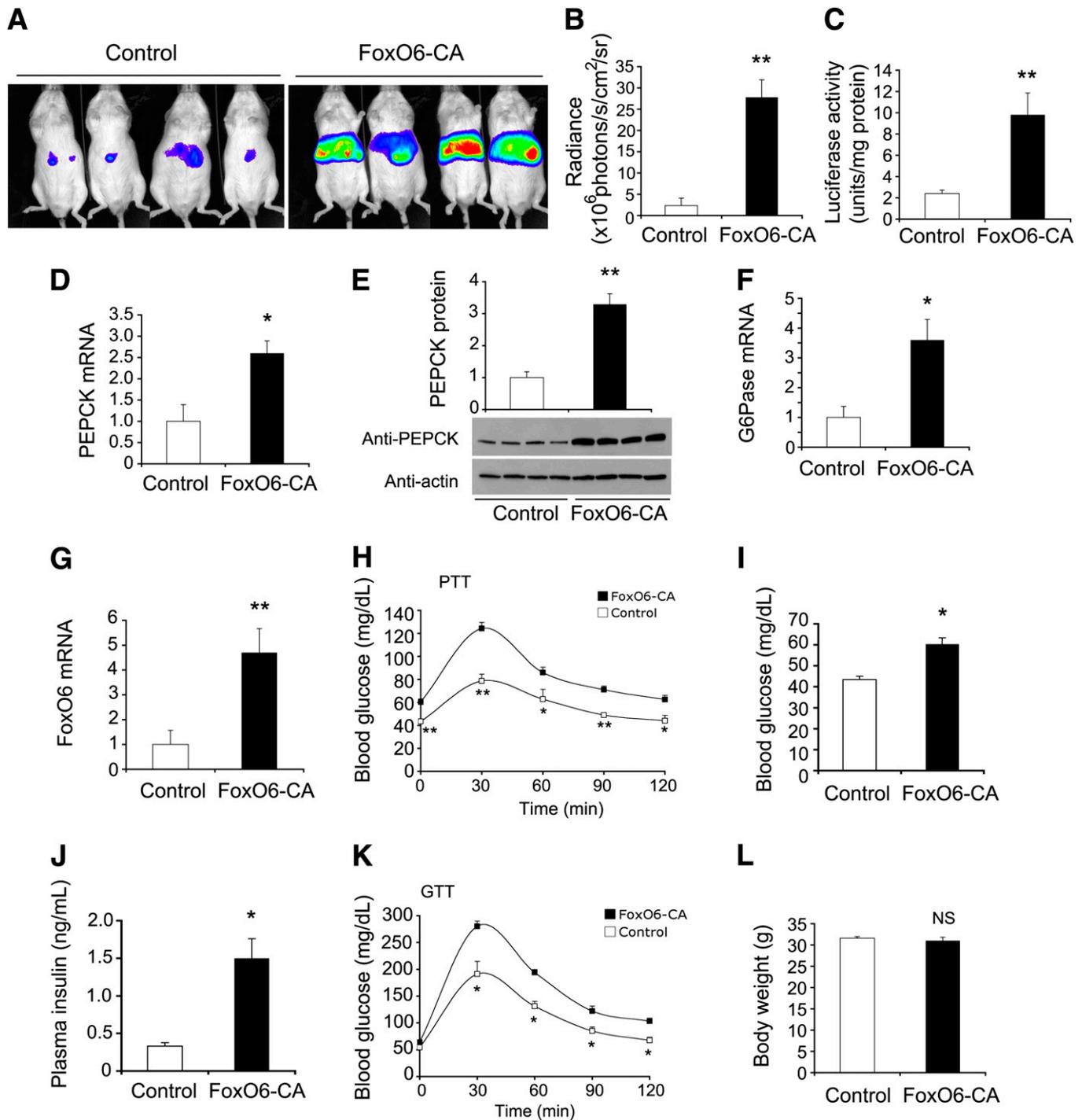
FIG. 3. Effect of FoxO6 gain-of-function on gluconeogenesis. CD1 male mice (aged 10 weeks) were stratified by body weight and randomly assigned to two groups ($n = 9$), which were intravenously injected with Adv-glucose-6-phosphate (G6P)-Luc vector (0.5×10^{11} plaque forming units [pfu]/kg) that is premixed with Adv-FoxO6-CA or Adv-null vector (1.5×10^{11} pfu/kg). *A*: Mice were injected 5 days after vector administration with a dose of D-luciferin (200 μg/g i.p.), followed by whole-body imaging. *B*: The mean radiance of mice, defined as the light unit (photons/s/cm²/sr [steradian]), was compared between FoxO6-CA and control groups. Mice were killed after 14 days of hepatic FoxO6-CA production. *C*: Liver tissues were subjected to luciferase activity assay for determining hepatic luciferase activity. Aliquots of liver tissues (20 mg) were analyzed for the determination of PEPCK mRNA (*D*), PEPCK protein (*E*), G6Pase mRNA (*F*), and FoxO6 mRNA levels (*G*). In parallel, two groups of CD1 mice ($n = 5$) were identically treated with FoxO6-CA or control vector, without the inclusion of the luciferase vector, for determining the effect of FoxO6-CA on glucose metabolism. *H*: Blood glucose profiles of the pyruvate tolerance test (PTT). Mice were fasted for 16 h, followed by an injection of pyruvate (2 g/kg i.p.). Blood glucose levels were measured before and after pyruvate infusion. Data were obtained after 8 days of hepatic FoxO6-CA production. *I*: Fasting blood glucose levels. *J*: Fasting plasma insulin levels. Mice were fasted for 16 h, followed by determination of fasting blood glucose levels. In addition, aliquots of blood (20 μL) were collected from individual mice for the determination of fasting plasma insulin levels. Data were obtained on day 5 after vector administration. *K*: Blood glucose profiles of glucose tolerance test (GTT). Mice were fasted for 16 h, followed by a glucose injection (2 g/kg i.p.). Blood glucose levels were measured before and after glucose infusion. Data were obtained after 5 days of hepatic FoxO6-CA production. *L*: Body weight. *$P < 0.05$ and **$P < 0.005$ vs. control by ANOVA; NS, not significant. (A high-quality digital representation of this figure is available in the online issue.)
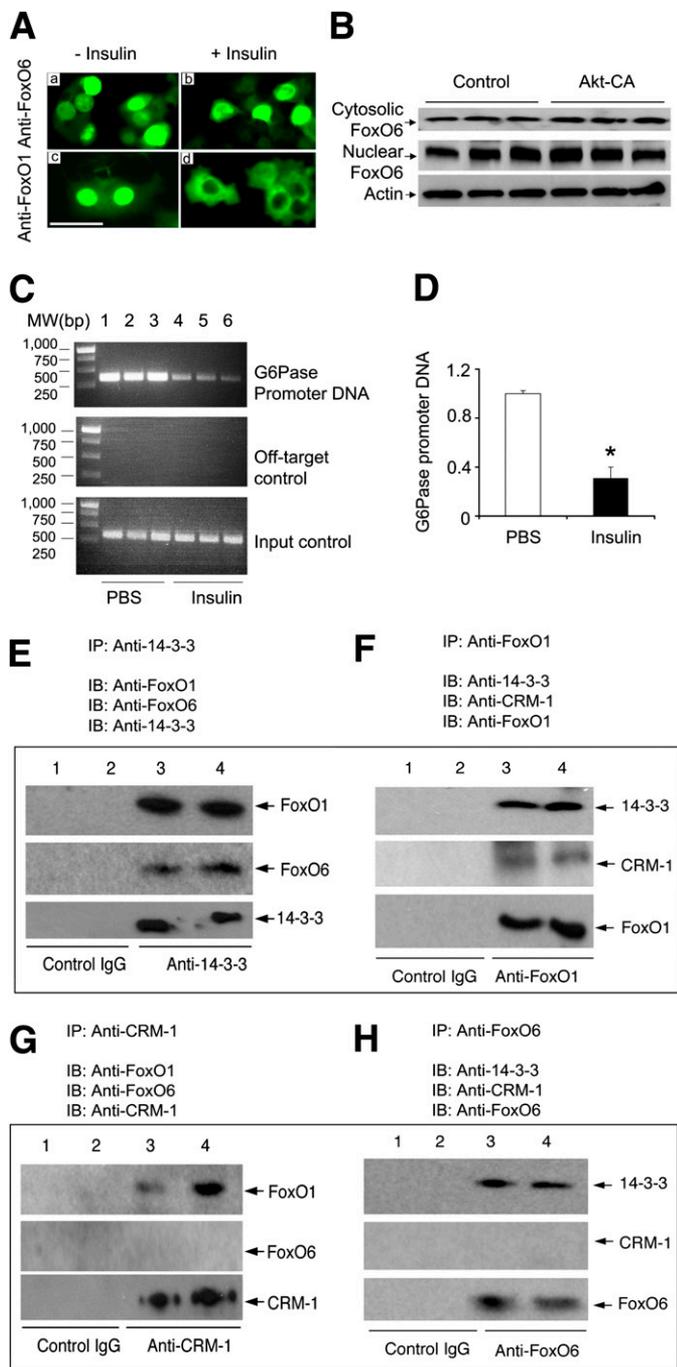
FIG. 4. FoxO6 subcellular distribution, DNA binding activity, and interaction with CRM-1. *A*: Immunohistochemistry. HepG2 cells pretransduced with 50 plaque forming units (pfu)/cell of FoxO6 vector (*a* and *b*) or FoxO1 vector (*c* and *d*) were serum-starved for 6 h, followed by incubation in the absence or presence of insulin (100 nmol/L) for 30 min. Cells were immunostained using rabbit anti-FoxO6 (*a*, *b*) or anti-FoxO1 (*c*, *d*) antibodies, followed by anti-rabbit IgG conjugated with fluorescein isothiocyanate (green). Bar = 25 μm. *B*: Immunoblot. HepG2 cells were transduced with 50 pfu/cell of FoxO6 vector in the absence or presence of Adv-Akt-CA vector (50 pfu/cell) expressing Akt-CA. After 24-h incubation, cells were harvested for the preparation of nuclear and cytoplasmic fractions, which were subjected to anti-FoxO6 immunoblot assay. *C*: Chromatin immunoprecipitation (ChIP) analysis of liver. C57BL/6J male mice (aged 10 weeks) were fasted for 16 h, followed by an injection of insulin (2 units/kg i.p.; *n* = 3) or phosphate-buffered saline (PBS; *n* = 3). Mice were killed 20 min after insulin injection, and aliquots of liver tissue (20 mg) underwent ChIP assay using rabbit anti-FoxO6 antibody for determining FoxO6 association with G6Pase promoter DNA. *D*: The amount of G6Pase promoter DNA bound by FoxO6 relative to input control DNA was determined in the liver of PBS- and insulin-treated mice. In addition, HepG2 cells were cotransduced with

of FoxO6 on hepatic G6Pase expression. This action was abolished in response to insulin injection into mice (Fig. 4*D*), suggesting that insulin-stimulated phosphorylation of FoxO6 disabled its cognate binding to the G6Pase promoter, resulting in loss of FoxO6 transcriptional activity.

To address the mechanism underlying the inability of FoxO6 to undergo insulin-dependent subcellular redistribution, we determined the association of FoxO6 with 14-3-3, a scaffold protein that is known to bind FoxO1 and modify its transcriptional activity (14). FoxO6 was shown to associate with 14-3-3, so was FoxO1, precluding the possibility that 14-3-3 is liable for the idiosyncrasy in protein trafficking between FoxO1 and FoxO6 (Fig. 4*E* and *F*). We then studied the interaction of FoxO6 with chromosome region maintenance (CRM-1), known as exportin-1, that is responsible for binding to the NES motif of a cargo protein and transporting the cargo protein from the nucleus to the cytoplasm (15,16). FoxO6 failed to interact with CRM-1 (Fig. 4*G* and *H*), coinciding with the absence of the NES motif in FoxO6. In contrast, FoxO1 was able to complex with CRM-1 (Fig. 4*F* and *G*), correlating with the presence of the NES motif in the carboxyl domain of FoxO1.

To underpin these findings, we treated HepG2 cells with leptomycin B, an agent that binds specifically to CRM-1 and inhibits its cargo-trafficking activity. As shown in Fig. 5, FoxO1 and CRM-1 were colocalized in the nucleus in the absence of insulin. In response to insulin, FoxO1, along with CRM-1, was translocated from the nucleus to the cytoplasm. Leptomycin B treatment abrogated the ability of FoxO1 to undergo insulin-elicited nuclear export. Like its wild-type counterpart, the FoxO6-CA mutant remained in the nucleus irrespective of insulin action (Supplementary Fig. 7). These data indicate that the incapability of FoxO6 to undergo insulin-dependent trafficking lies in its inability to interact with CRM-1.

Effect of FoxO6 gain-of-function on glucose metabolism. To determine the contribution of FoxO6 to glucose metabolism, we generated transgenic mice expressing the constitutively active FoxO6-CA allele from the liver-specific transthyretin promoter. This transgenic line expressed FoxO6-CA specifically in the liver, with nondetectable expression in other peripheral tissues, including pancreatic β-cells (Supplementary Fig. 8). Male FoxO6-CA transgenic mice exhibited significantly higher fasting blood glucose levels compared with control littermates (Fig. 6*A*). This effect correlated with increased hepatic expression of PEPCK (Fig. 6*B*), G6Pase (Fig. 6*C*), and FoxO6 (Fig. 6*D*) in the livers of FoxO6-CA transgenic mice. FoxO6-CA transgenic mice developed glucose intolerance (Fig. 6*E*), accompanied by fasting hyperinsulinemia (Fig. 6*F*). These impaired blood glucose profiles were persistently observed in FoxO6-CA transgenic mice at different ages (Supplementary Fig. 9). No differences in body weights (Fig. 6*G*) or insulin tolerance tests (Fig. 6*H*) were detected between FoxO6 transgenic mice and control littermates.

FoxO1 and FoxO6 vectors at a fixed dose (50 pfu/cell). **P* < 0.005 vs. control by ANOVA. After a 24-h incubation, cells were collected for the preparation of total protein lysates, which were subjected to immunoprecipitation using anti–14-3-3 (*E*), anti-FoxO1 (*F*), anti–CRM-1 (*G*), or anti-FoxO6 antibody (*H*). The control antibody was anti–β-galactosidase IgG. The immunoprecipitates were analyzed for the presence of FoxO1, FoxO6, 14-3-3, or CRM-1. IB, immunoblotting; IP, immunoprecipitation; MW, molecular weight; bp, base pair. (A high-quality digital representation of this figure is available in the online issue.)
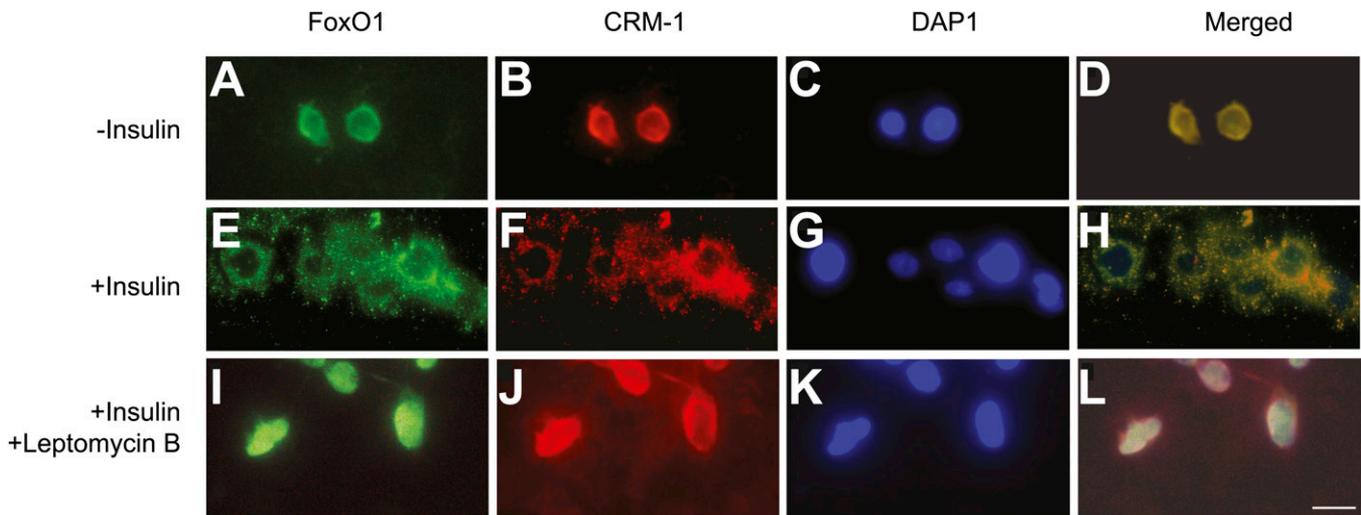
FIG. 5. CRM-1 mediates insulin-dependent FoxO1 trafficking. HepG2 cells were transduced with FoxO1 vector at a fixed dose (50 plaque forming units/cell). After 24-h incubation, cells were serum-starved for 6 h, followed by treatment with insulin (100 nmol/L) in the absence or presence of leptomycin B (10 nmol/L) in culture medium for 30 min, followed by immunohistochemistry using anti-FoxO1 and anti–CRM-1 antibodies. FoxO1 was localized predominantly within the nucleus in the absence of insulin (*A–D*). In response to insulin, FoxO1 and CRM-1 were translocated from the nucleus to cytoplasm (*E–H*). This insulin-stimulated FoxO1 trafficking was abolished by leptomycin B (*I–L*), an agent that binds specifically to CRM-1 and disables the ability of CRM-1 to transport its cargo protein from the nucleus to the cytoplasm. (A high-quality digital representation of this figure is available in the online issue.)

Likewise, no significant differences were seen in levels of nonfasting blood glucose, nonfasting plasma insulin, and glucagon between FoxO6 transgenic mice and age- and sex-matched littermate controls (Supplementary Fig. 10). To assess the effect of FoxO6-CA on hepatic gluconeogenesis, we used the pyruvate tolerance test to assess the ability of the liver to convert pyruvate to glucose. FoxO6-CA transgenic mice displayed significantly higher blood glucose levels (Fig. 6*I*), correlating with elevated G6Pase activity (Fig. 6*J*). These data indicate that FoxO6 gain-of-function augmented gluconeogenesis in the liver.

Effect of FoxO6 loss-of-function on glucose metabolism. To further illustrate the importance of FoxO6 in gluconeogenesis, we used the siRNA-mediated gene-silencing approach to knock down FoxO6 expression in the liver. This approach generated a liver-specific FoxO6-deficient model. The FoxO6-deficient mice ($n = 10$) exhibited significantly reduced fasting blood glucose levels (Fig. 7*A*). Hypoglycemia (blood glucose <50 mg/dL) developed in ~50% after a 24-h fast, indicating that FoxO6 loss-of-function was associated with impaired ability to maintain fasting euglycemia during prolonged fasting. This effect correlated with near depletion of hepatic FoxO6 expression (Fig. 7*B* and *C*) and significant reduction in hepatic G6Pase activity (Fig. 7*D*), G6Pase mRNA (Fig. 7*E*), PEPCK mRNA (Fig. 7*F*), and PEPCK protein (Fig. 7*G*) expression in FoxO6-siRNA vector-treated mice. Hepatic FoxO1 expression remained unchanged in FoxO6-siRNA vector-treated mice (Fig. 7*H*), confirming the specificity of FoxO6-siRNA for selective FoxO6 knockdown in the liver. Likewise, no significant impact of FoxO6-siRNA on hepatic FoxO3 and FoxO4 expression was seen in FoxO6-siRNA vector-treated mice versus the control group (Supplementary Fig. 11). Furthermore, no differences in body weight (Fig. 7*I*) and liver enzyme levels (Supplementary Fig. 11) were detected, ruling out the possibility that the reduction in blood glucose levels was the result of hepatotoxicity in FoxO6-siRNA vector-treated mice. Mice with hepatic FoxO6 depletion displayed lower fasting insulin levels (Fig. 7*J*),

secondary to reduced hepatic gluconeogenesis. This was validated by pyruvate tolerance test. FoxO6-deficient mice exhibited significantly lower blood glucose levels after the intraperitoneal pyruvate injection (Fig. 7*K*), suggesting that FoxO6 depletion was associated with diminished hepatic gluconeogenesis.

To reinforce this interpretation, we transferred the FoxO6-siRNA vector into mouse primary hepatocytes. FoxO6 depletion halved the capacity of hepatocytes to produce glucose in response to cAMP/dexamethasone stimulation (Fig. 7*L*), consistent with the idea that loss of FoxO6 function attenuates the ability of the liver to undergo gluconeogenesis, contributing to fasting hypoglycemia in FoxO6-deficient mice.

FoxO6 inhibition ameliorates fasting hyperglycemia in diabetes. To assess the functional contribution of FoxO6 to the pathogenesis of fasting hyperglycemia in diabetes, we used the siRNA-mediated gene-silencing approach to ablate FoxO6 expression in diabetic *db/db* mice. From our observation that FoxO6 became deregulated, accounting for its augmented activity in promoting gluconeogenesis in the insulin-resistant liver (Fig. 1), we hypothesized that selective FoxO6 inhibition would curb excessive gluconeogenesis in the insulin-resistant liver and improve glucose metabolism in diabetes.

To test this hypothesis, we stratified diabetic *db/db* mice by body weight and fasting blood glucose levels into two groups, which were treated with FoxO6-siRNA or scrambled Sc-siRNA vector. Compared with age- and sex-matched heterozygous *db/+* littermates ($n = 8$), diabetic *db/db* mice ($n = 7$) exhibited fasting hyperglycemia (Fig. 8*A*) and hyperinsulinemia (Fig. 8*B*), accompanied by glucose intolerance (Fig. 8*C*). These metabolic abnormalities were significantly improved in FoxO6-siRNA vector-treated *db/db* mice ($n = 7$) (Fig. 8*A–C*). Furthermore, *db/db* mice in the FoxO6-siRNA groups displayed significantly improved blood glucose profiles in response to insulin tolerance (Fig. 8*D*).

To address the underlying mechanism, we determined the effect of FoxO6 knockdown on hepatic gluconeogenesis,
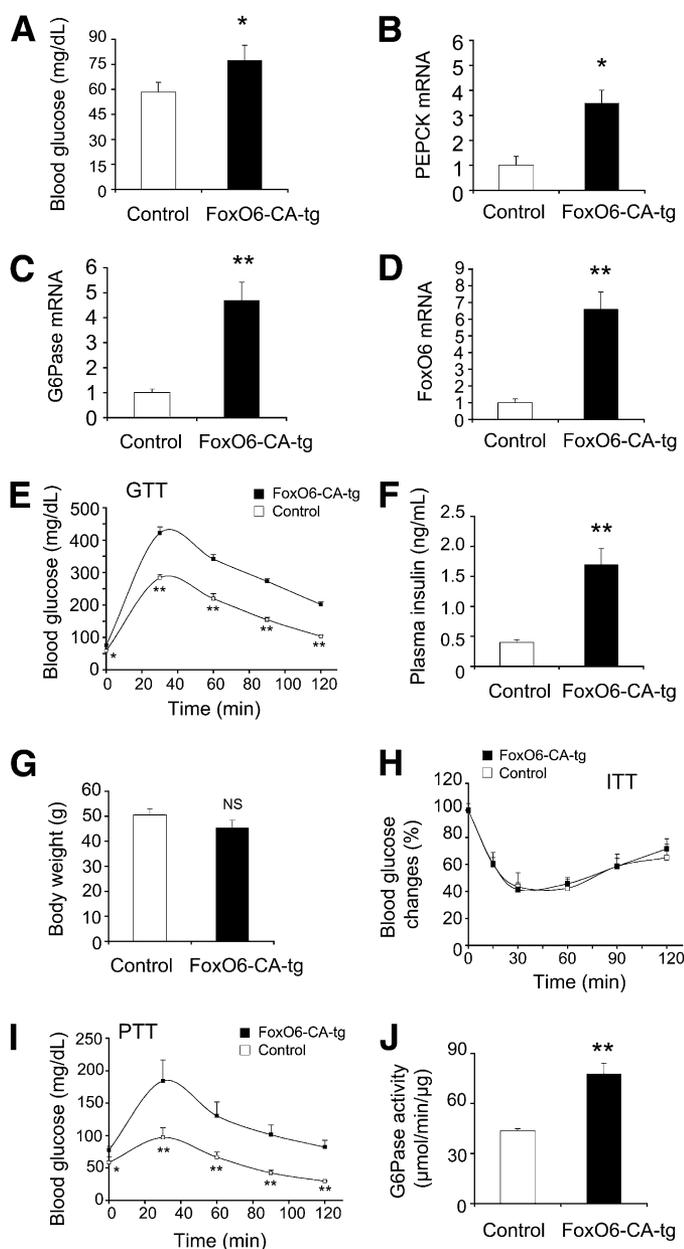
FIG. 6. Effect of FoxO6 transgenic expression on glucose metabolism. FoxO6-CA transgenic (FoxO6-CA-tg) and wild-type littermates were characterized for glucose metabolism. *A*: Blood glucose levels were determined after a 16-h fast. *B*: Hepatic PEPCK mRNA levels. *C*: Hepatic G6Pase mRNA levels. *D*: Hepatic FoxO6 mRNA levels. *E*: Blood glucose profiles of glucose tolerance tests (GTT). Mice were fasted for 16 h, followed by glucose injection (2 g/kg i.p. body wt). Blood glucose levels were measured before and after glucose injection. *F*: Plasma insulin levels were determined after a 16-h fast. *G*: Body weight. *H*: Blood glucose profiles of insulin tolerance tests (ITT). Mice were injected with insulin (0.75 IU/kg i.p.), followed by determination of blood glucose levels. *I*: Blood glucose profiles of pyruvate tolerance tests (PTT). Mice were fasted for 16 h, followed by injection of pyruvate (2 g/kg i.p. body wt). Blood glucose levels were measured before and after pyruvate injection. *J*: Hepatic G6Pase activity. All data were obtained from male FoxO6-CA-tg mice ($n = 8–10$) and male age-matched (aged 49–40 weeks) control littermates ($n = 5–8$). $*P < 0.05$ and $**P < 0.005$ vs. control by ANOVA; NS, not significant.

demonstrating that hepatic G6Pase activity (Fig. 8*E*), along with hepatic G6Pase (Fig. 8*F*) and PEPCK (Fig. 8*G*) mRNA levels, was significantly reduced in FoxO6-siRNA vector-treated *db/db* mice. These effects were attributable to siRNA-mediated FoxO6 depletion in the liver, because

hepatic FoxO6 mRNA levels were reduced to basal levels in FoxO6-siRNA vector-treated *db/db* mice (Fig. 8*H*). In contrast, no significant impact of hepatic FoxO6-siRNA production on FoxO1 mRNA abundance (Fig. 8*I*) or body weight (Fig. 8*J*) was detectable in diabetic *db/db* mice. These data highlight the significance of hepatic FoxO6 deregulation in the pathogenesis of fasting hyperglycemia, validating the concept that selective FoxO6 inhibition in the insulin-resistant liver contributed to the suppression of hepatic gluconeogenesis and amelioration of fasting hyperglycemia in diabetic *db/db* mice.

DISCUSSION

Our studies characterize FoxO6 as a novel transcription factor that independently mediates insulin action on hepatic gluconeogenesis. We demonstrate in cultured hepatocytes and multiple animal models that FoxO6 gain-of-function promoted gluconeogenesis in the liver and that this effect was inhibited by insulin. Under physiologic conditions, hepatic FoxO6 activity was enhanced in response to fasting, and this action served to prime the liver for augmented gluconeogenesis for maintaining blood glucose levels within the physiologic range. In response to postprandial insulin secretion, hepatic FoxO6 activity is inhibited, serving as an acute mechanism for curbing hepatic glucose production to prevent excessive postprandial glucose excursion. In insulin-resistant states, hepatic FoxO6 expression became deregulated because of an impaired ability of insulin to keep hepatic FoxO6 activity in check. This effect contributed in part to unrestrained hepatic gluconeogenesis and fasting hyperglycemia in diabetes. Consistent with this interpretation, we demonstrate that selective FoxO6 knockdown in the insulin-resistant liver was capable of suppressing hepatic gluconeogenesis and improving blood glucose profiles in diabetic *db/db* mice. From these significant findings, we conclude that FoxO6 plays a critical and nonredundant role in mediating insulin-dependent regulation of gluconeogenesis in the liver.

Our studies, together with previous data (1,2), indicate that insulin signaling bifurcates downstream of Akt/PKB to two parallel checkpoints, namely FoxO1 and FoxO6, for controlling hepatic gluconeogenesis in response to insulin. This begets a fundamental question: Why does the liver evolve two parallel routes (FoxO1 and FoxO6) for adjusting the rate of hepatic glucose production in response to insulin? Our interpretation is that these two parallel pathways operate in a complementary manner, such that one will compensate for functional loss of the other. This dual mechanism provides double security for ensuring the functional integrity of the liver for efficient metabolic adaptation from fasting to feeding states, because inept response of the liver to insulin consequently results in hepatic glucose overproduction—a chief contributing factor for fasting hyperglycemia in diabetes.

Although classified to the FoxO family, FoxO6 is evolutionarily diverged from other FoxO members (Supplementary Fig. 12). FoxO6 (640 amino acid residues) displays the least homology ($<30\%$) in amino acid sequence with FoxO1 (652 amino acid residues), contains only two Akt/PKB phosphorylation sites (Thr[26] and Ser[184]), and lacks the NES, a structural motif that is conserved in the carboxyl domain of other members of the FoxO family. Here, we show that FoxO6 deviates from FoxO1 in orchestrating insulin action on target gene expression. Although FoxO6 is phosphorylated in response to insulin, phosphorylated
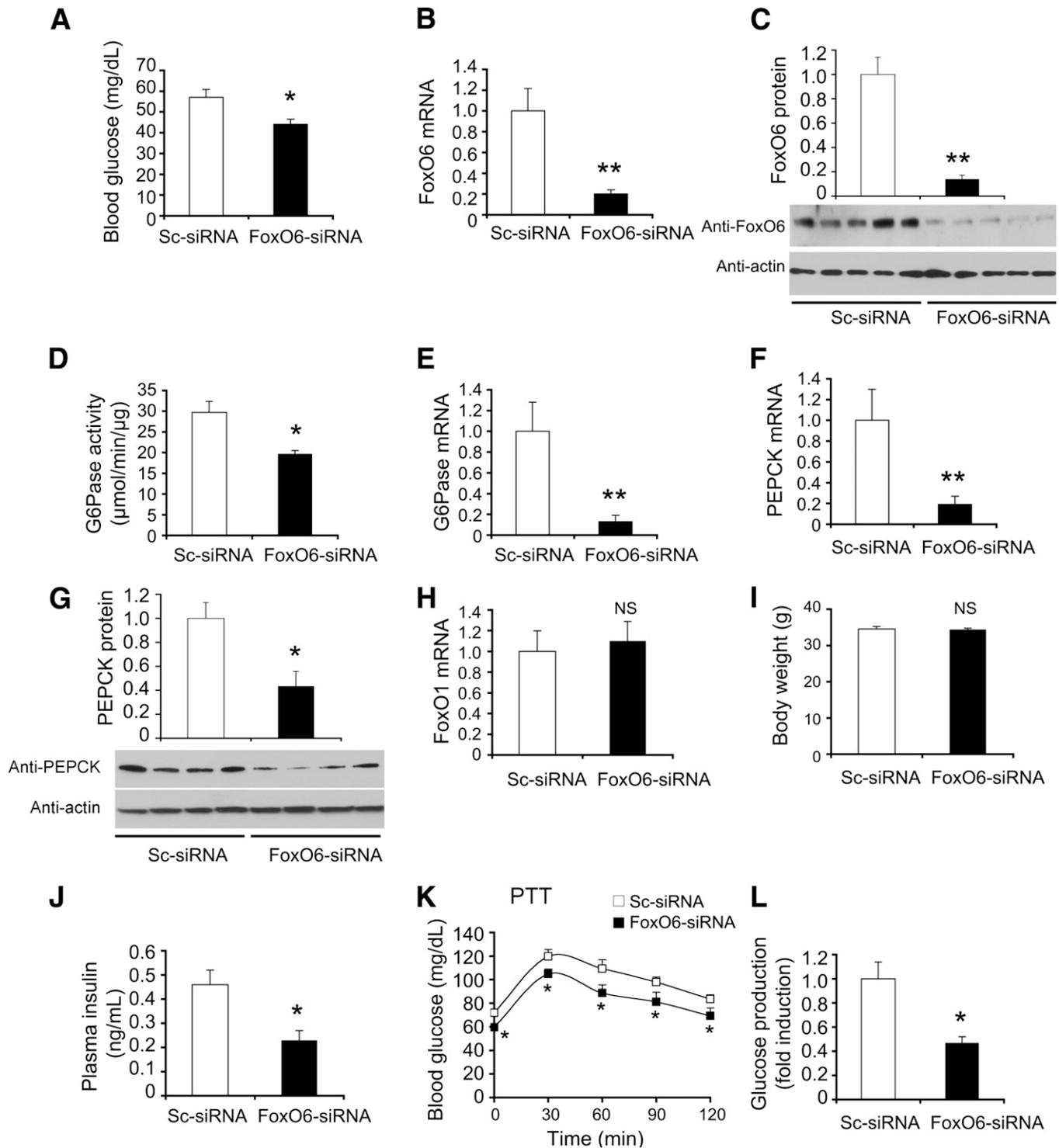
FIG. 7. Effect of FoxO6 loss of function on gluconeogenesis. CD1 male mice (aged 10 weeks) were stratified by body weight and randomly assigned to two groups (n = 10), which were intravenously injected with a predefined dose (1.5×10^{11} plaque forming units [pfu]/kg) of Adv-FoxO6-siRNA vector expressing FoxO6-specific siRNA under the U6 promoter or control Adv-Sc-siRNA vector encoding scrambled siRNA under the U6 promoter. A: Blood glucose levels. B: Hepatic FoxO6 mRNA levels. C: Hepatic FoxO6 protein levels. D: Hepatic G6Pase activity. E: Hepatic G6Pase mRNA levels. F: Hepatic PEPCK mRNA levels. G: Hepatic PEPCK protein levels. H: Hepatic FoxO1 mRNA levels. I: Body weight. J: Plasma insulin levels. K: Blood glucose profiles of pyruvate tolerance tests (PTT). Blood glucose and plasma insulin levels were determined after a 16-h fast at day 10 after vector administration. PTT was performed at day 14. Mice were killed after a 16-h fast after 15 days of hepatic FoxO6-siRNA expression. Liver tissues were subjected to real-time quantitative RT-PCR analysis and G6Pase activity assay. L: Glucose production in FoxO6-deficient hepatocytes. Mouse primary hepatocytes (2×10^5 cells/well in 12-well microplates) were treated with Adv-FoxO6-siRNA or Adv-Sc-siRNA vector at the dose of 100 pfu/cell in the presence of 8-cpt-cAMP (cAMP analog, 500 μmol/L) and dexamethasone (100 μmol/L). Each condition was run in six replicates. After 24-h incubation, the amount of glucose released from hepatocytes into culture medium was determined between FoxO6-siRNA and control Sc-siRNA groups. $*P$ < 0.05 and $**P$ < 0.005 vs. control by ANOVA; NS, not significant.
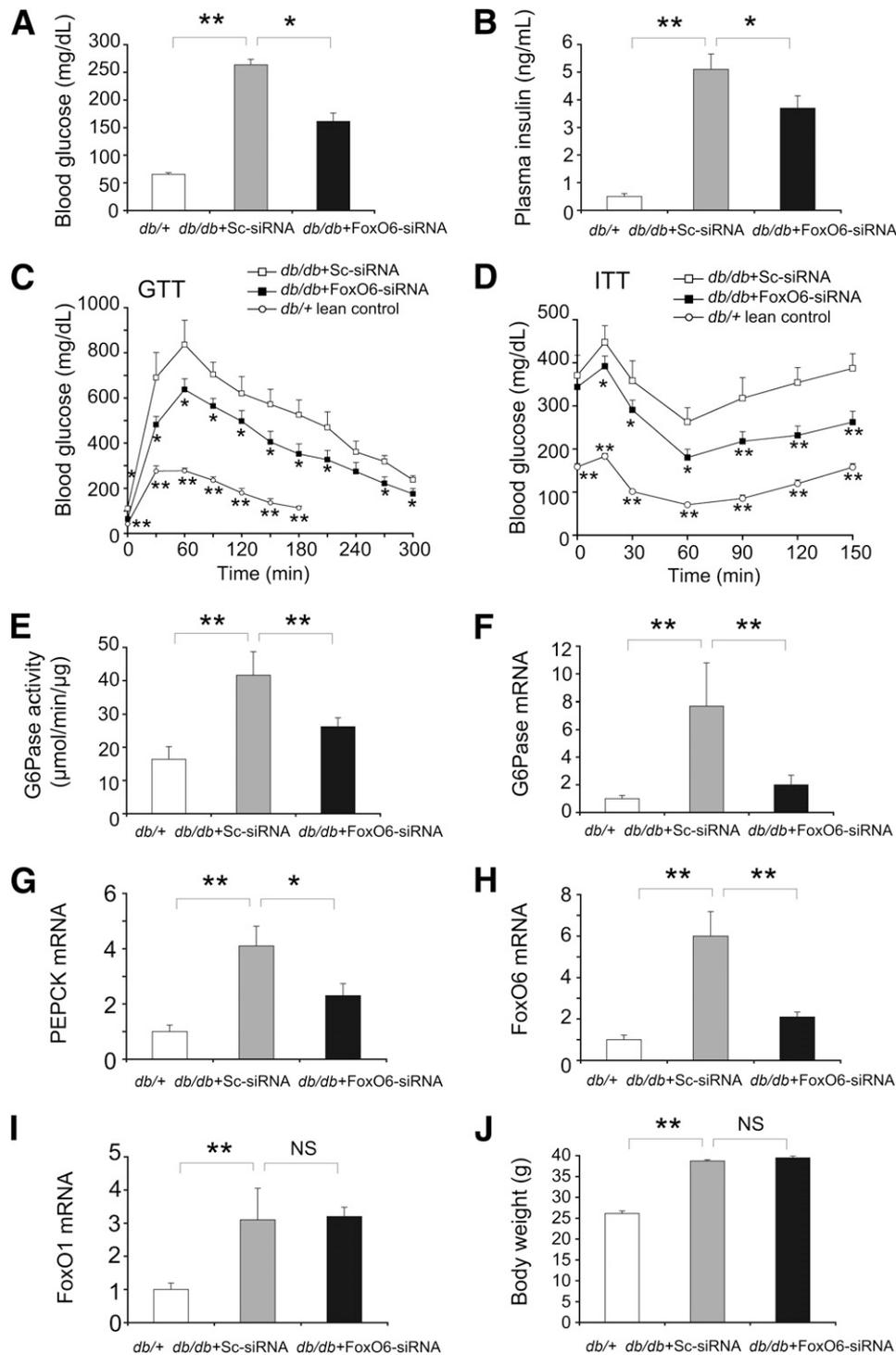
FIG. 8. Beneficial effect of FoxO6 inhibition on glucose metabolism in diabetes. Diabetic male *db/db* mice (aged 12 weeks) were stratified by body weight and fasting blood glucose levels and randomly assigned to two groups (*n* = 7), which were treated with 1.5×10^{11} plaque forming units of FoxO6-siRNA or Sc-siRNA control vector. One group of male age-matched heterozygous *db/+* littermates (*n* = 8) was used as a normal control. *A*: Blood glucose levels. *B*: Plasma insulin levels. After 5 days of vector administration, mice were fasted for 16 h, followed by the determination of blood glucose and plasma insulin levels. *C*: Blood glucose profiles in response to glucose tolerance test (GTT). After a 16-h fast, mice were injected with glucose (3 g/kg i.p.), followed by the determination of blood glucose levels. Data were obtained from day 5, and similar results were reproduced at day 10 after vector administration. *D*: Blood glucose profiles in response to insulin tolerance test (ITT). Mice were injected with insulin (2 IU/kg i.p.) at day 10 after vector administration, followed by determination of blood glucose levels. *E*: Hepatic G6Pase activity. *F*: Hepatic G6Pase mRNA levels. *G*: Hepatic PEPCK mRNA levels. *H*: Hepatic FoxO6 mRNA levels. *I*: Hepatic FoxO1 mRNA levels. *J*: Body weight. Mice were killed at day 12 after vector administration, and liver tissues were collected for the determination of hepatic G6Pase activity and hepatic mRNA levels corresponding to G6Pase, PEPCK, FoxO6, and FoxO1 by real-time quantitative RT-PCR assay using β-actin mRNA as control. *$P < 0.05$ and **$P < 0.005$ vs. control by ANOVA; NS, not significant.

FoxO6 does not undergo insulin-dependent trafficking from the nucleus to the cytoplasm in hepatocytes. This finding is recapitulated in HEK293 cells, in which FoxO6 is confined to the nucleus, regardless of insulin action (17). Interestingly, FoxO6 is sensitive to insulin inhibition in hepatocytes. This is evidenced by the abolition of FoxO6-mediated induction of G6Pase promoter activity in the presence of insulin. These data illustrate a distinct mechanism by which FoxO6 mediates insulin action on target gene expression without altering its subcellular distribution.

One interpretation is that insulin induces FoxO6 phosphorylation and distorts its DNA-binding domain, preventing FoxO6 from binding to target promoters. In support of this notion, we demonstrate that insulin acutely inhibited FoxO6 transcriptional activity by disabling its cognate binding to target gene promoters in the liver. Alternatively, phosphorylation of FoxO6 promotes its association with other factors, such as the multifunctional factor 14-3-3, which masks the FoxO6 DNA-binding domain and precludes FoxO6 binding to target promoters. Two lines of evidence support this interpretation. First, FoxO6 contains a consensus 14-3-3 binding motif (^{23}RSCTWP^{28}) within its DNA-binding domain. Second, we show that FoxO6 is able to complex with 14-3-3 in the nucleus of hepatocytes. Our data consolidate the idea that 14-3-3, which is present in both nucleus and cytoplasm, participates in post-translational modification of FoxO activity (14,18–23), consistent with the idea that insulin inhibition of FoxO transcriptional activity and FoxO nucleocytoplasmic trafficking are two distinct events.

To our knowledge, this is the first in-depth characterization of FoxO6 in glucose metabolism. We show that FoxO6 is ubiquitously expressed, defying an earlier observation that FoxO6 is predominantly expressed in the brain (24). Importantly, our studies reveal a distinct route by which the liver orchestrates insulin-dependent regulation of gluconeogenesis, underscoring the physiologic importance of insulin signaling through FoxO6 in the liver for fine-tuning hepatic gluconeogenesis in response to the metabolic shift from fasting to feeding states. Unlike other members of FoxO family, FoxO6 mediates insulin action in a distinct mechanism, without altering its subcellular redistribution. Our findings that FoxO6 activity becomes unchecked in the insulin-resistant liver and that FoxO6 inhibition ameliorates fasting hyperglycemia in diabetic mice provide the proof-of-concept that selective FoxO6 inhibition is beneficial for curbing excessive hepatic glucose production and improving glycemic control in diabetes.

REFERENCES

1. Accili D, Arden KC. FoxOs at the crossroads of cellular metabolism, differentiation, and transformation. Cell 2004;117:421–426
2. Barthel A, Schmoll D, Unterman TG. FoxO proteins in insulin action and metabolism. Trends Endocrinol Metab 2005;16:183–189
3. Sparks JD, Sparks CE. Overindulgence and metabolic syndrome: is FoxO1 a missing link? J Clin Invest 2008;118:2012–2015
4. Puigserver P, Rhee J, Donovan J, et al. Insulin-regulated hepatic gluconeogenesis through FOXO1-PGC-1alpha interaction. Nature 2003;423:550–555
5. Kamagate A, Dong HH. FoxO1 integrates insulin signaling to VLDL production. Cell Cycle 2008;7:3162–3170
6. Matsumoto M, Pocai A, Rossetti L, Depinho RA, Accili D. Impaired regulation of hepatic glucose production in mice lacking the forkhead transcription factor Foxo1 in liver. Cell Metab 2007;6:208–216
7. Kamagate A, Qu S, Perdomo G, et al. FoxO1 mediates insulin-dependent regulation of hepatic VLDL production in mice. J Clin Invest 2008;118:2347–2364
8. Rodgers JT, Haas W, Gygi SP, Puigserver P. Cdc2-like kinase 2 is an insulin-regulated suppressor of hepatic gluconeogenesis. Cell Metab 2010;11:23–34
9. Haeusler RA, Kaestner KH, Accili D. FoxOs function synergistically to promote glucose production. J Biol Chem 2010;285:35245–35248
10. Qu S, Altomonte J, Perdomo G, et al. Aberrant Forkhead box O1 function is associated with impaired hepatic metabolism. Endocrinology 2006;147:5641–5652
11. Altomonte J, Cong L, Harbaran S, et al. Foxo1 mediates insulin action on apoC-III and triglyceride metabolism. J Clin Invest 2004;114:1493–1503
12. Foretz M, Hébrard S, Leclerc J, et al. Metformin inhibits hepatic gluconeogenesis in mice independently of the LKB1/AMPK pathway via a decrease in hepatic energy state. J Clin Invest 2010;120:2355–2369
13. Bernal-Mizrachi E, Wen W, Stahlhut S, Welling CM, Permutt MA. Islet beta cell expression of constitutively active Akt1/PKB alpha induces striking hypertrophy, hyperplasia, and hyperinsulinemia. J Clin Invest 2001;108:1631–1638
14. Zhao X, Gan L, Pan H, et al. Multiple elements regulate nuclear/cytoplasmic shuttling of FOXO1: characterization of phosphorylation- and 14-3-3-dependent and -independent mechanisms. Biochem J 2004;378:839–849
15. Monecke T, Güttler T, Neumann P, Dickmanns A, Görlich D, Ficner R. Crystal structure of the nuclear export receptor CRM1 in complex with Snurportin1 and RanGTP. Science 2009;324:1087–1091
16. Dong X, Biswas A, Süel KE, et al. Structural basis for leucine-rich nuclear export signal recognition by CRM1. Nature 2009;458:1136–1141
17. van der Heide LP, Jacobs FM, Burbach JP, Hoekman MF, Smidt MP. FoxO6 transcriptional activity is regulated by Thr26 and Ser184, independent of nucleo-cytoplasmic shuttling. Biochem J 2005;391:623–629
18. Brunet A, Kanai F, Stehn J, et al. 14-3-3 transits to the nucleus and participates in dynamic nucleocytoplasmic transport. J Cell Biol 2002;156:817–828
19. Brent MM, Anand R, Marmorstein R. Structural basis for DNA recognition by FoxO1 and its regulation by posttranslational modification. Structure 2008;16:1407–1416
20. Silhan J, Vacha P, Strnadova P, et al. 14-3-3 protein masks the DNA binding interface of forkhead transcription factor FOXO4. J Biol Chem 2009;284:19349–19360
21. Zhang X, Gan L, Pan H, et al. Phosphorylation of serine 256 suppresses transactivation by FKHR (FOXO1) by multiple mechanisms. Direct and indirect effects on nuclear/cytoplasmic shuttling and DNA binding. J Biol Chem 2002;277:45276–45284
22. Woods YL, Rena G. Effect of multiple phosphorylation events on the transcription factors FKHR, FKHRL1 and AFX. Biochem Soc Trans 2002;30:391–397
23. Bridges D, Moorhead GB. 14-3-3 proteins: a number of functions for a numbered protein. Sci STKE 2004;2004:re10
24. Jacobs FM, van der Heide LP, Wijchers PJ, Burbach JP, Hoekman MF, Smidt MP. FoxO6, a novel member of the FoxO class of transcription factors with distinct shuttling dynamics. J Biol Chem 2003;278:35959–35967